Electronic Supplementary Material (ESI) for Physical Chemistry Chemical Physics.

Ionic Ir(III) Complex-Interfacial Layer for Efficient Carrier Collection via Induced Electric Dipole

Minsoo Lee ‡[ab] Hyun-Tak Kim, ‡[abc] Ji Hoon Seo, ‡[de] HyeonOh Shin,[ab] Febrian Tri Adhi Wibowo,[d] Sung-Yeon Jang, *[df] Kwanyong Seo *[df] and Tae-Hyuk Kwon *[abfg]

a. Department of Chemistry, Ulsan National Institute of Science and Technology (UNIST), Ulsan 44919, Republic of Korea

b. Center for Wave Energy Materials, Ulsan National Institute of Science and Technology (UNIST), Ulsan 44919, Republic of Korea

c. Center for Environment & Sustainable Resources, Korea Research Institue of Chemical Technology (KRICT), Daejeon 34114, Republic of Korea

d. School of Energy and Chemical Engineering, Ulsan National Institute of Science and Technology (UNIST), Ulsan 44919, Republic of Korea

e. New & Renewable Energy Laboratory, Korea Electric Power Research Institute (KEPRI), Daejeon 34056, Republic of Korea

f. Graduate School of Carbon Neutrality, Ulsan National Institute of Science and Technology (UNIST), Ulsan 44919, Korea

g. Graduate School of Semiconductor Materials and Device Engineering, Ulsan National Institute of Science and Technology (UNIST), Ulsan 44919, Republic of Korea

‡ These authors contributed equally.

Synthesis and characterization, XRD, GI-WAXD, device performance, IPCE, stability test and XPS depth profile, Scheme 1-4, Fig. S1-19, and Table S1-4.

Contents

1. Synthesis and characterization

In this study, 2-phenylquinoline (2pq, 1) was chosen as the main ligand in the iridium complexes because iridium (III) complex with 2pq ligand exhibited high absorption coefficient in UV region in previous studies.

Scheme 1

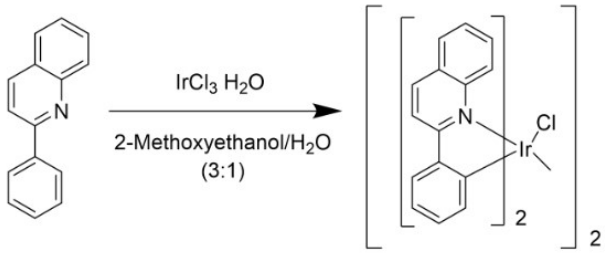

1 **2**

Compound 2: A mixture of $IrCl_3 \cdot H_2O$ (500 mg, 1.68 mmol) and 2-phenylquinoline (700 mg, 3.41 mmol) was refluxed for 24 h in a 3:1 mixture of 2-methoxyethanol and water. After cooling to room temperature, more water added to precipitate the product. The resulting mixture was subsequently filtered through a Buchner funnel and then washed with hexane and ethyl ether several times to yield the crude product (700 mg, 62.7% yield).

Scheme 2

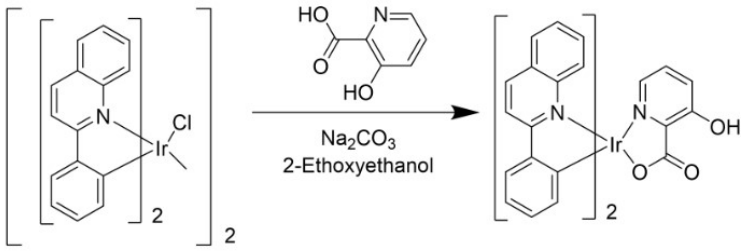

2 **3**

Compound 3: A mixture of compound 2 (500 mg, 0.393 mmol), 3-hydroxypicolinic acid (164 mg, 1.68 mmol) and Na_2CO_3 (417 mg, 3.93 mmol) was refluxed in an inert (N_2) atmosphere for 10-12 h in 2-ethoxyethanol. After cooling to room temperature, the solvent was evaporated in high vacuum and dissolved in methylene chloride. The organic phase was washed with water and dried over $MgSO_4$. The solvent was evaporated to give the crude product, which was applied to column chromatography on silica gel, followed by eluting with methylene chloride and methyl alcohol (10:1, v/v) to provide the desired product (420 mg, 72.3% yield).

^{1}H NMR (400 MHz, DMSO): δ (ppm) 13.45 (s, 1H), 8.68 (d, 1H), 8.24 (d, 1H), 8.22 (d, 1H), 8.14 (m, 2H), 7.98 (dd, 1H), 7.87 (dd, 1H), 7.77 (m, 2H), 7.58 (m, 1H), 7.50 (m, 2H), 7.39 (m, 2H), 7.15 (m, 2H), 7.13 (m, 1H), 7.01 (m, 1H), 6.98 (m, 1H), 6.89 (m, 1H), 6.80 (m, 1H), 6.69 (m, 1H), 6.31 (dd, 1H).

Scheme 3

3 **4**

Compound 4: A mixture of compound 3 (500 mg, 0.67 mmol), Cs_2CO_3 (440 mg, 1.35 mmol) and 1,4-butanesultone (644 mg, 4.73 mmol) in DMF was stirred at room temperature for 24 h. The solvent was evaporated in vacuum and dissolved in methylene chloride. The organic phase was washed with water, brine and dried over $MgSO_4$. The solvent was evaporated to give the crude product, which was applied to column chromatography on silica gel, eluting with methylene chloride and methyl alcohol (10:1, v/v) to provide the desired product (200 mg, 33% yield), whose spectroscopic data were identical with the reported.[2]

Fig. S1. ^{1}H NMR of Product 4 in DMSO

^{1}H NMR (400 MHz, DMSO): δ (ppm) 8.80 (d, 1H), 8.52 (m, 5H), 8.22 (d, 1H), 8.03 (t, 2H), 7.96 (d, 1H), 7.49 (m, 6H), 7.30 (d, 1H), 7.05 (q, 2H), 6.95 (t, 1H), 6.70 (t, 1H), 6.60 (m, 2H), 6.07 (d, 1H), 3.80 (m, 2H), 2.38 (t, 2H), 1.56 (m, 4H).

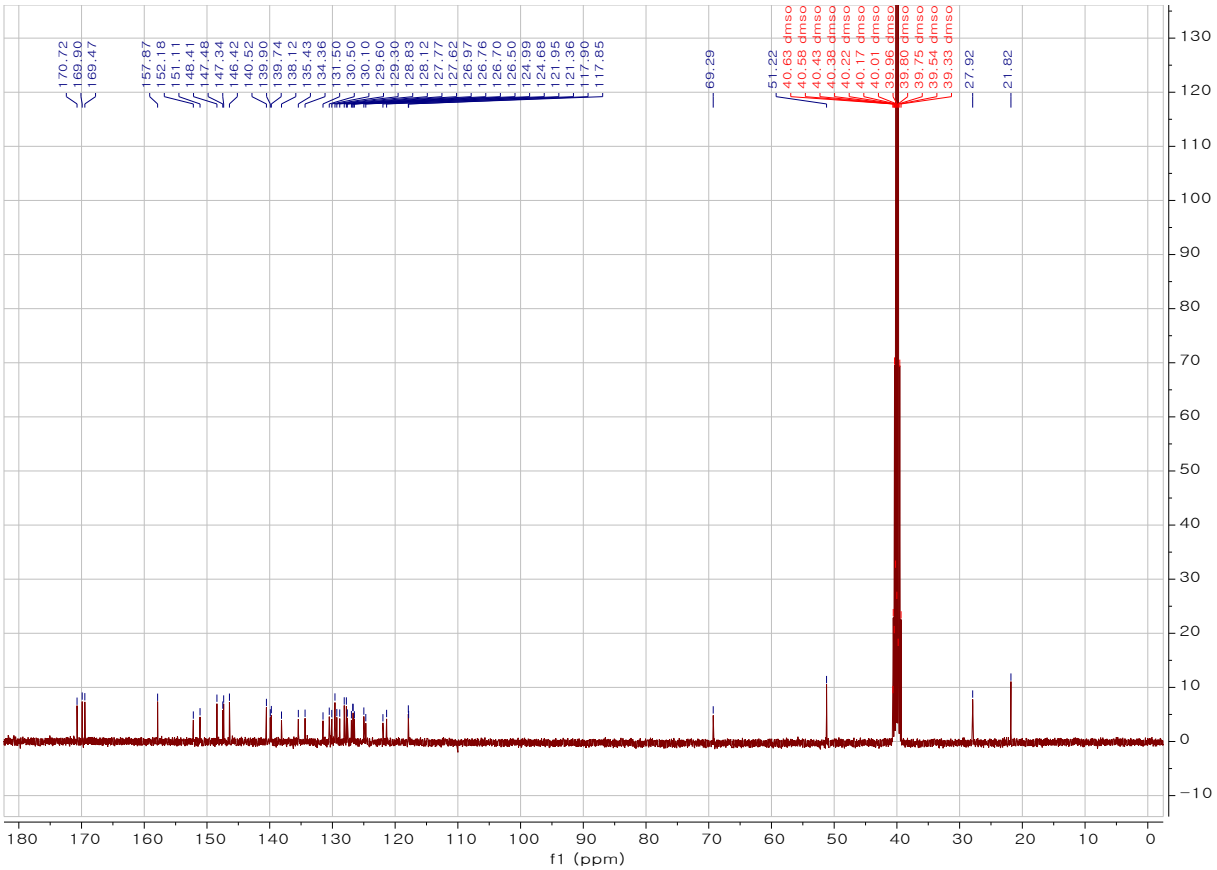

Fig. S2. ^{13}C NMR of Product 4 in DMSO

^{13}C NMR (125 MHz, DMSO): 170.72, 169.90, 169.47, 157.87, 152.18, 151.11, 148.41, 147.48, 147.34, 146.42, 140.52, 139.90, 139.74, 138.12, 136.43, 134.36, 131.50, 130.50, 130.10, 129.60, 129.30, 129.30, 128.83, 128.12, 127.77, 127.63, 126.97, 126.76, 126.70, 126.50, 124.99, 124.68, 121.95, 121.36, 117.90, 117.85, 69.29, 51.22, 27.92, 21.82.

Scheme 4

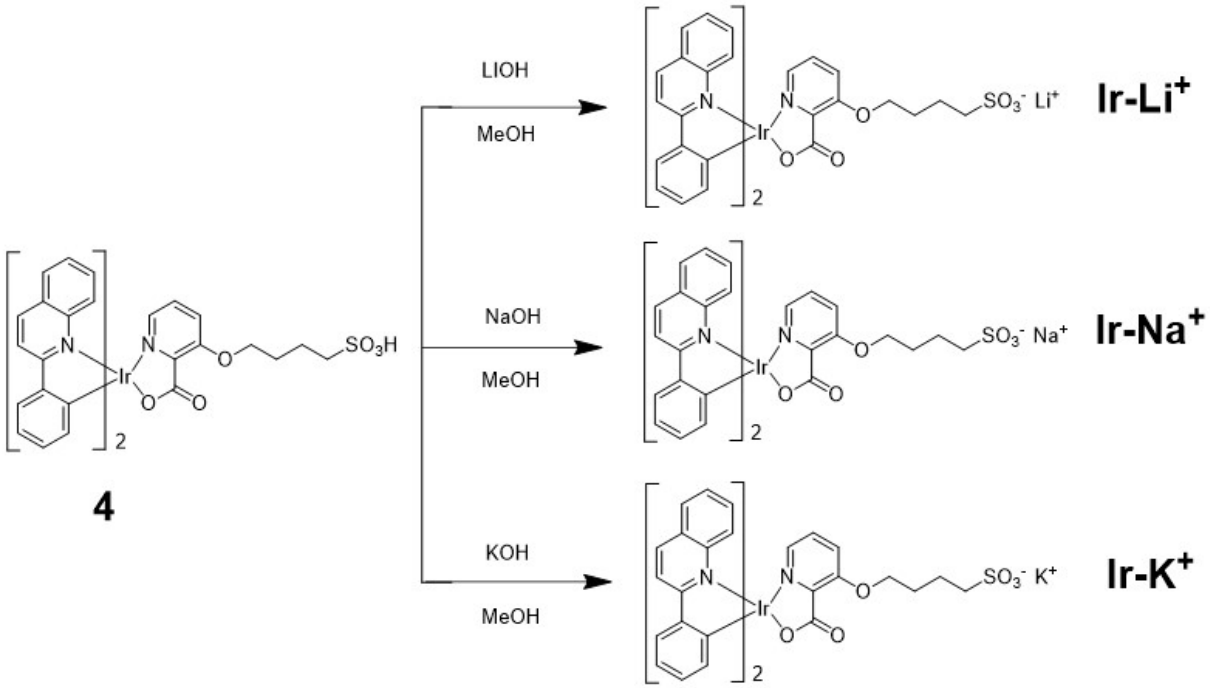

Ir-Li^+, Ir-Na^+, and Ir-K^+: A mixture of compound 4 (200 mg, 0.11 mmol) and LiOH or NaOH or KOH (10 mg, 0.26 mmol) in methyl alcohol was stirred for 24 h at room temperature. The solvent was evaporated to give the orange-red solid, which was recrystallized in dichloromethane and hexane (180 mg, 88% yield).

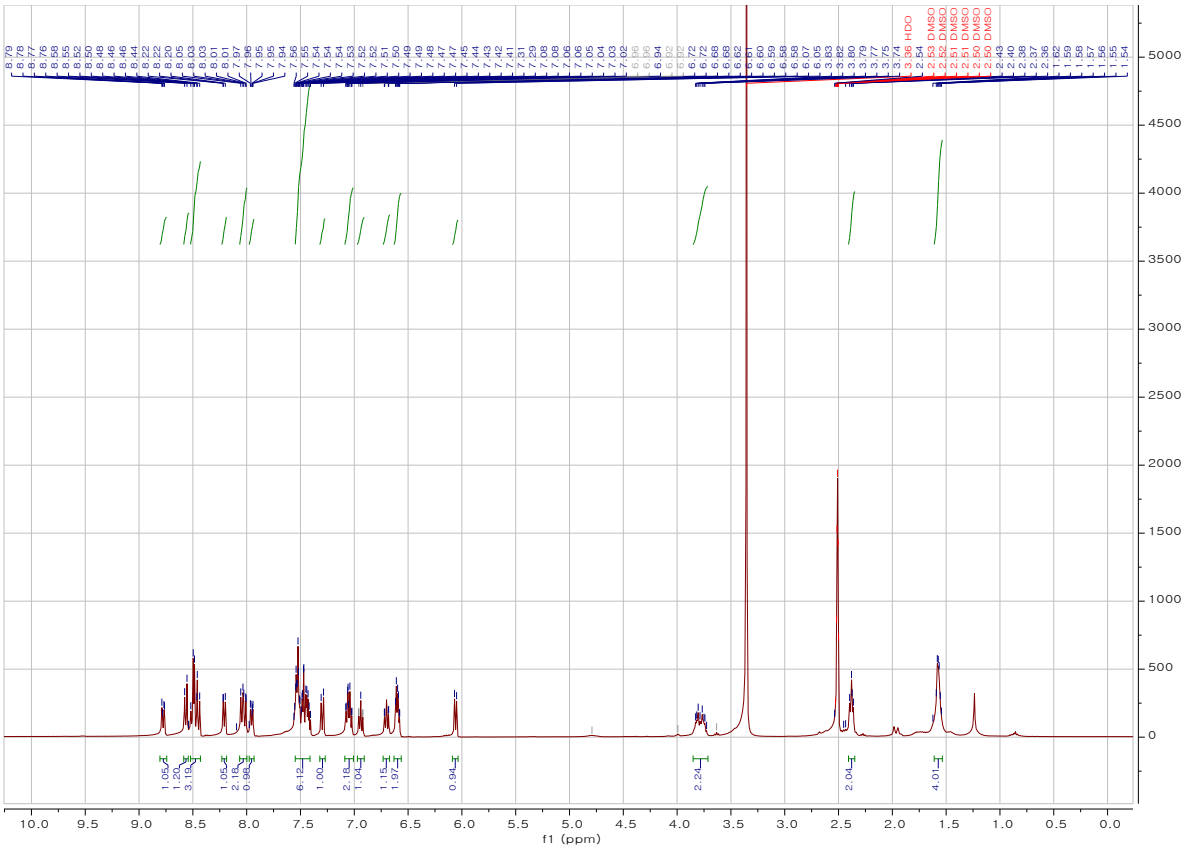

Fig. S3. ^{1}H NMR of Ir-Li^{+} in DMSO.

^{1}H NMR (400 MHz, DMSO): δ (ppm) 8.78 (d, 1H), 8.55 (d, 1H), 8.48 (q, 3H), 8.22 (d, 1H), 8.03 (t, 2H), 7.96 (d, 1H), 7.48 (m, 6H), 7.30 (d, 1H), 7.05 (q, 2H), 6.94 (t, 1H), 6.70 (t, 1H), 6.60 (m, 2H), 6.07 (d, 1H), 3.78 (m, 2H), 2.38 (t, 2H), 1.57 (m, 4H).

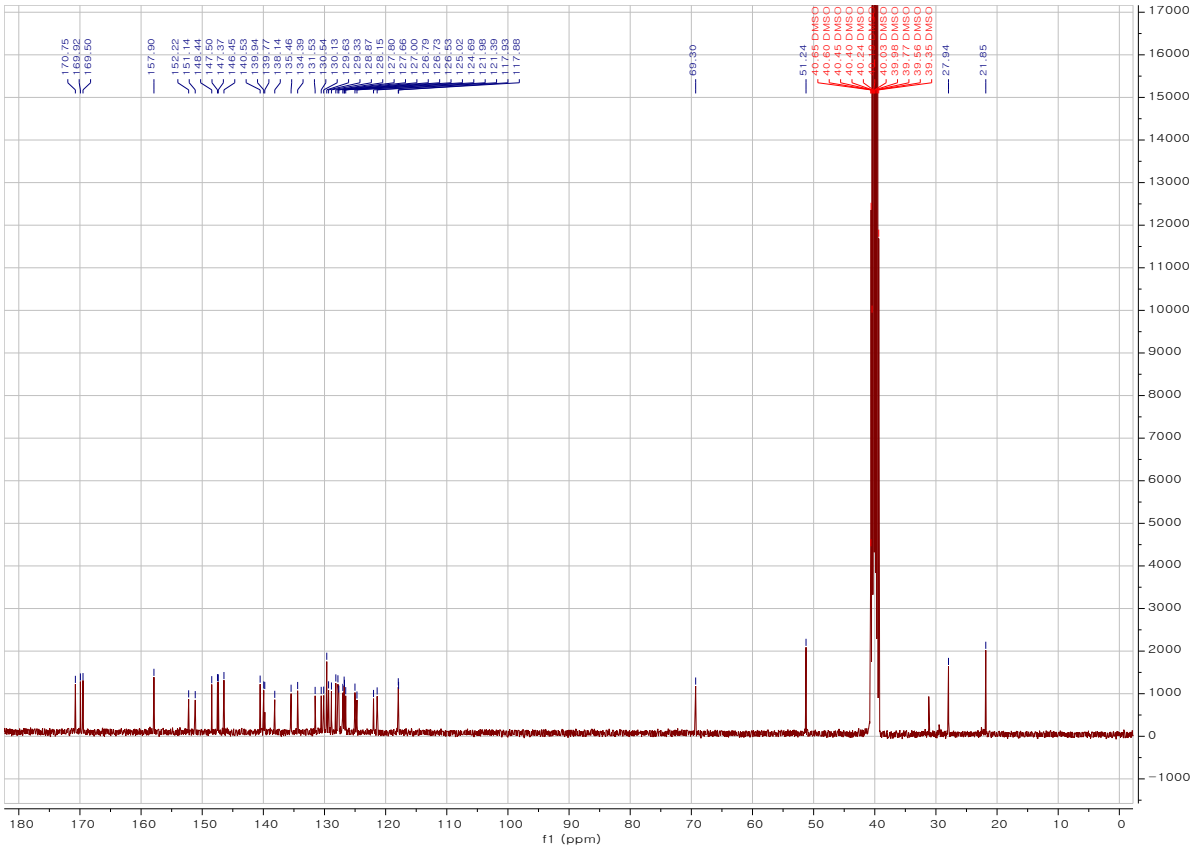

Fig. S4. ^{13}C NMR of Ir-Li^{+} in DMSO.

^{13}C NMR (125 MHz, DMSO): δ (ppm) 170.75, 169.92, 169.50, 157.90, 152.22, 151.14, 148.44, 147.50, 147.37, 146.45, 140.53, 139.94, 139.77, 138.14, 135.46, 134.39, 131.53, 130.54, 130.13, 129.63, 128.87, 128.15, 127.80, 127.66, 127.00, 126.79, 126.73, 126.53, 125.02, 124.69, 121.98, 121.39, 117.93, 117.88, 69.30, 51.24, 27.94, 21.85.

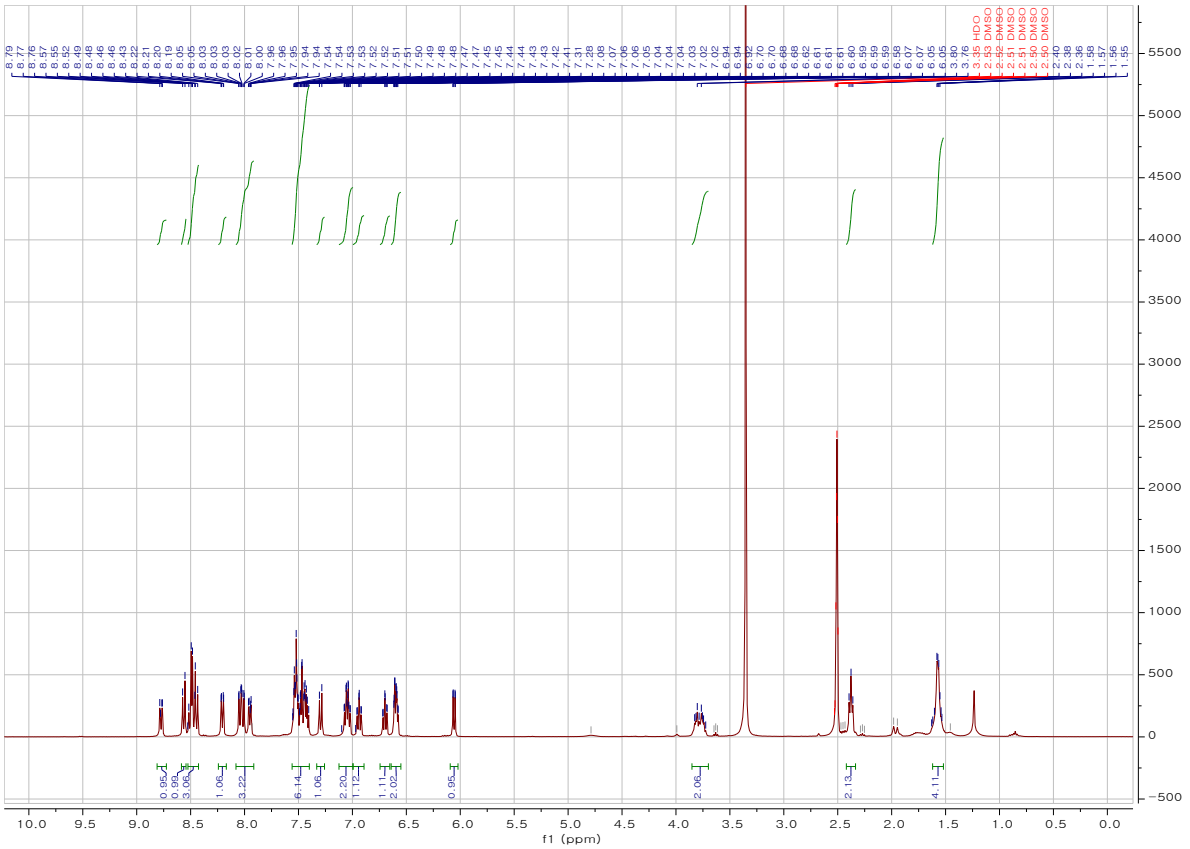

Fig. S5. ^{1}H NMR of Ir-Na^{+} in DMSO.

^{1}H NMR (400 MHz, DMSO): δ (ppm) 8.78 (d, 1H), 8.55 (d, 1H), 8.48 (q, 3H), 8.22 (d, 1H), 8.03 (t, 2H), 7.96 (d, 1H), 7.48 (m, 6H), 7.30 (d, 1H), 7.05 (q, 2H), 6.94 (t, 1H), 6.70 (t, 1H), 6.60 (m, 2H), 6.07 (d, 1H), 3.78 (m, 2H), 2.38 (t, 2H), 1.57 (m, 4H).

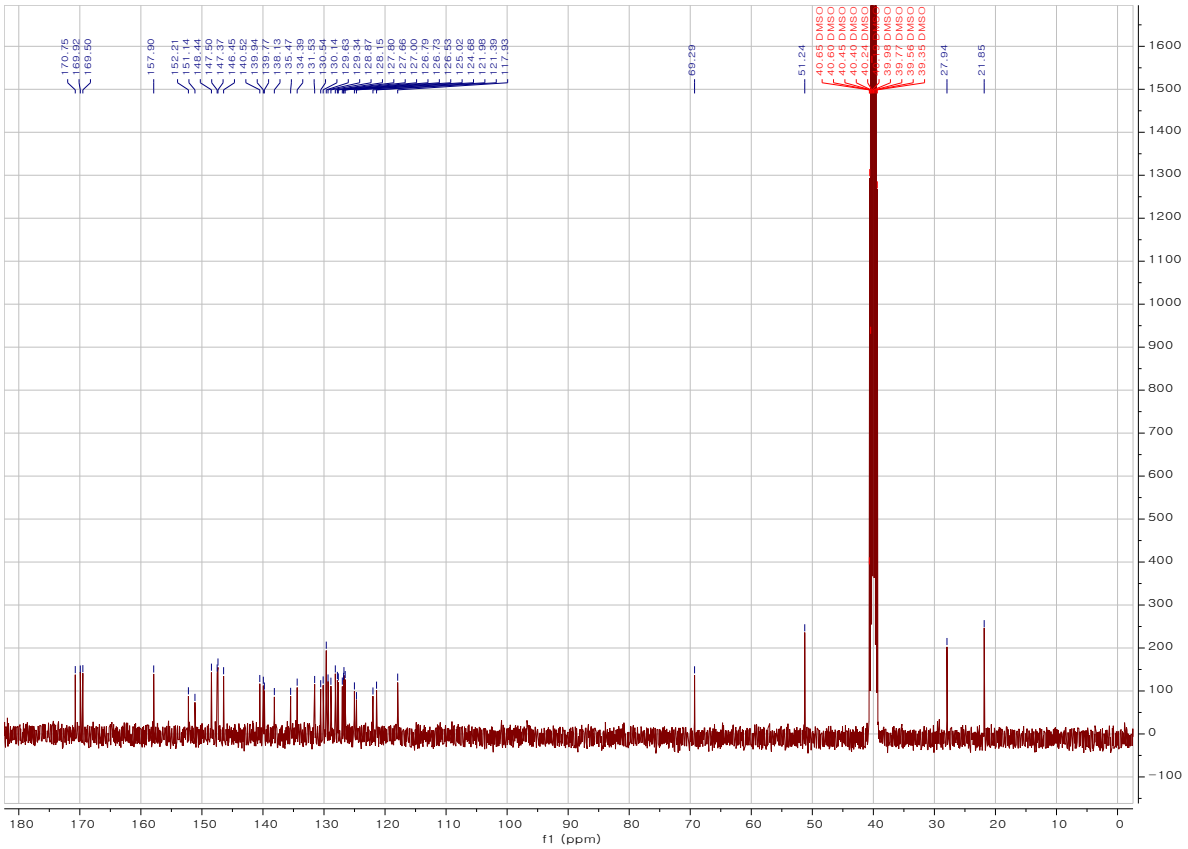

Fig. S6. ^{13}C NMR of Ir-Na^+ in DMSO.

^{13}C NMR (125 MHz, DMSO): δ (ppm) 170.75, 169.92, 169.50, 157.90, 152.21, 151.14, 148.44, 147.50, 147.37, 146.45, 140.52, 139.94, 139.77, 138.13, 135.47, 134.39, 131.53, 130.54, 130.14, 129.63, 129.34, 128.87, 128.15, 127.80, 127.66, 127.00, 126.79, 126.73, 126.53, 125.02, 124.68, 121.98, 121.39, 117.93, 69.29, 51.24, 27.94, 21.85.

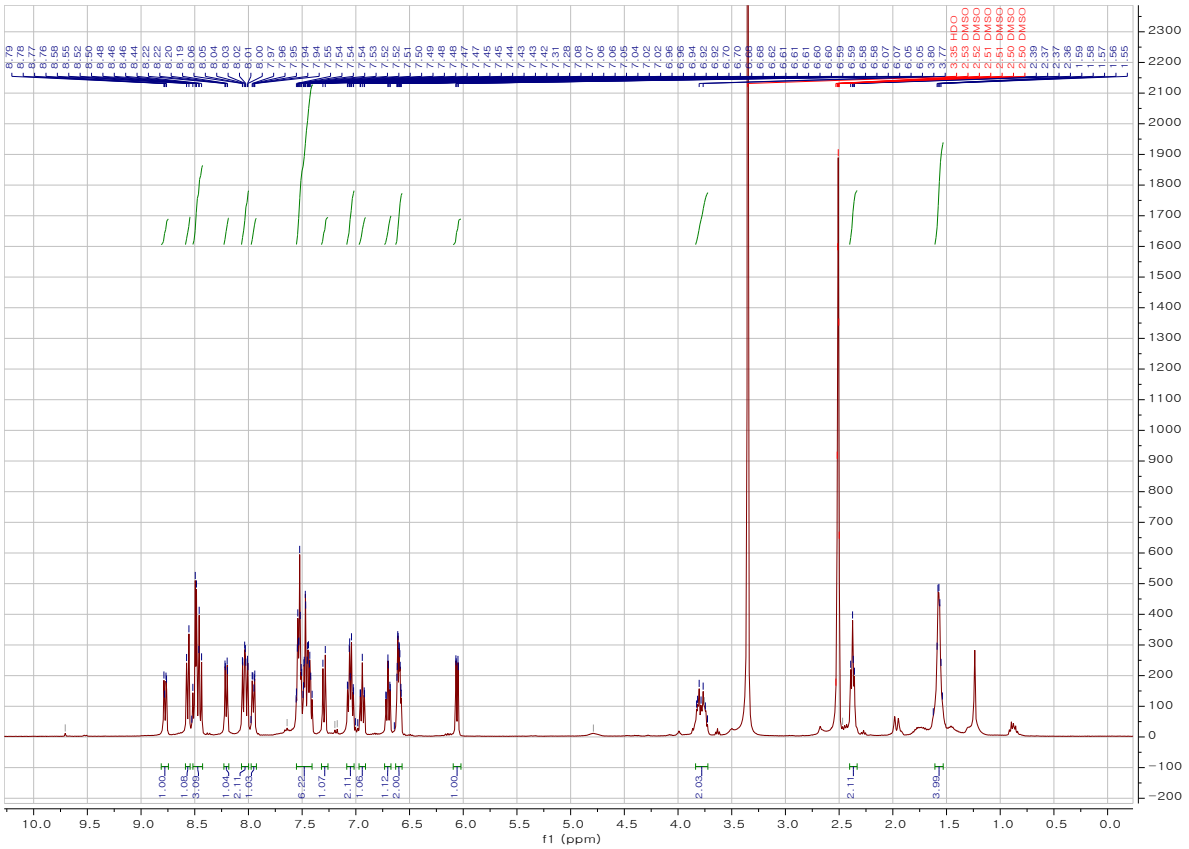

Fig. S7. ^{1}H NMR of Ir-K^{+} in DMSO.

^{1}H NMR (400 MHz, DMSO): δ (ppm) 8.78 (d, 1H), 8.55 (d, 1H), 8.48 (q, 3H), 8.22 (d, 1H), 8.03 (t, 2H), 7.96 (d, 1H), 7.48 (m, 6H), 7.30 (d, 1H), 7.05 (q, 2H), 6.94 (t, 1H), 6.70 (t, 1H), 6.60 (m, 2H), 6.07 (d, 1H), 3.78 (m, 2H), 2.38 (t, 2H), 1.57 (m, 4H).

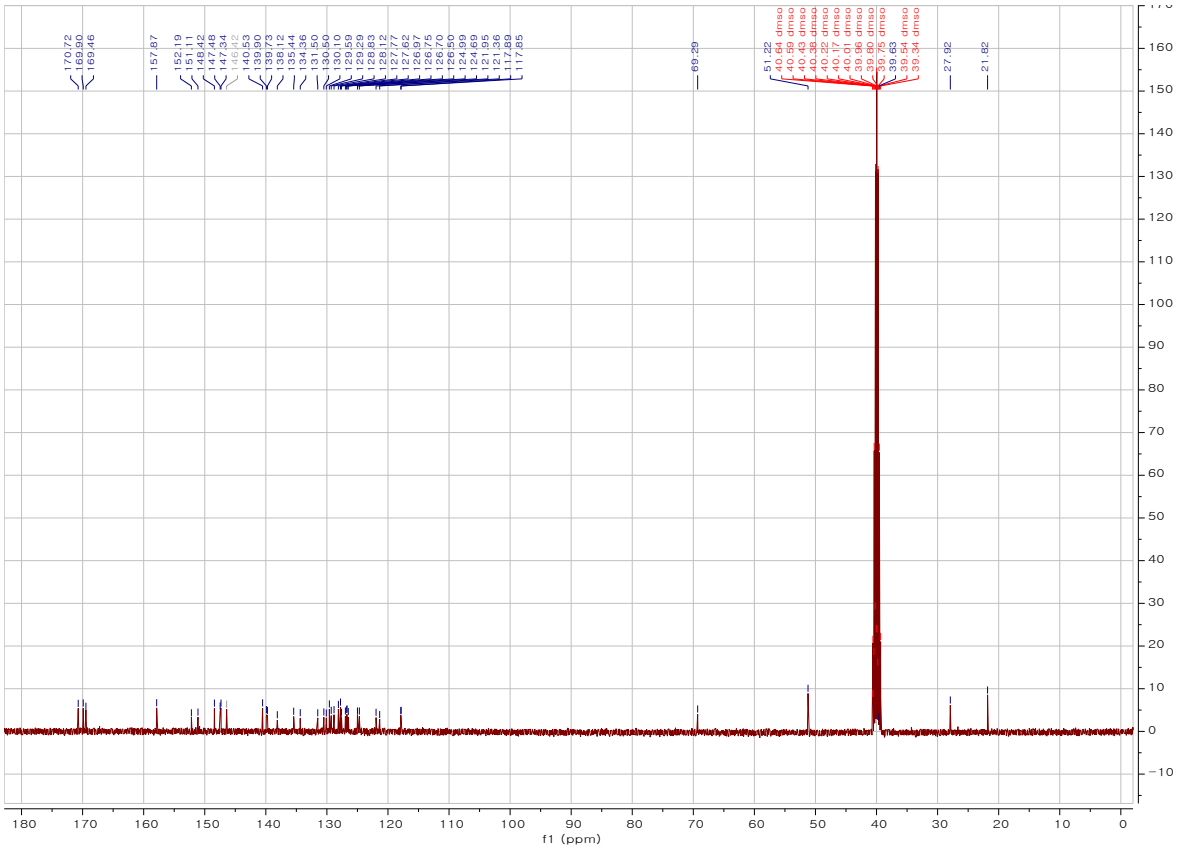

Fig. S8. ^{13}C NMR of Ir-K^+ in DMSO.

^{13}C NMR (125 MHz, DMSO): 170.72, 169.90, 169.47, 157.87, 152.18, 151.11, 148.41, 147.48, 147.34, 146.42, 140.52, 139.90, 139.74, 138.12, 136.43, 134.36, 131.50, 130.50, 130.10, 129.60, 129.30, 129.30, 128.83, 128.12, 127.77, 127.63, 126.97, 126.76, 126.70, 126.50, 124.99, 124.68, 121.95, 121.36, 117.90, 117.85, 69.29, 51.22, 27.92, 21.82.

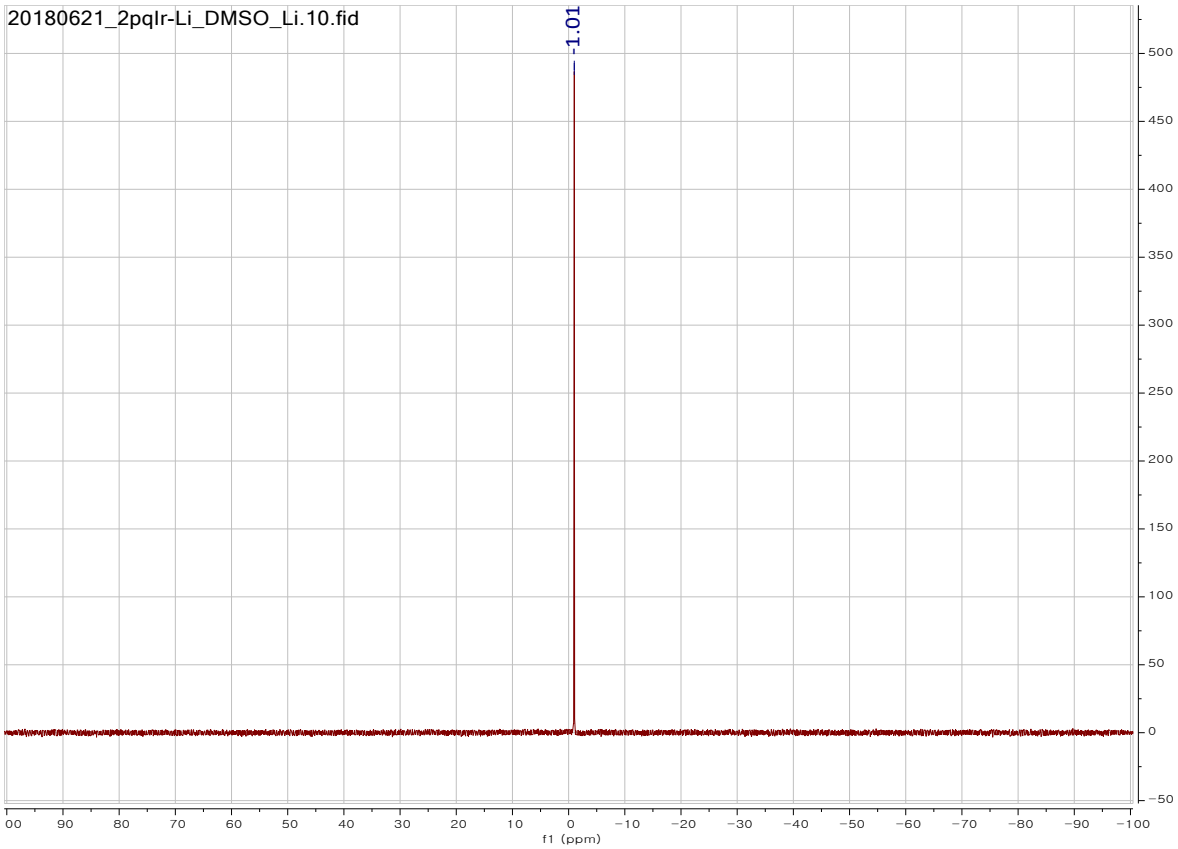

Fig. S9. ^{7}Li-NMR spectrum of Ir-Li^{+}.

^{7}Li-NMR spectrum of Ir-Li^{+} show peak at -1.01 ppm, which correspond to Li salts.

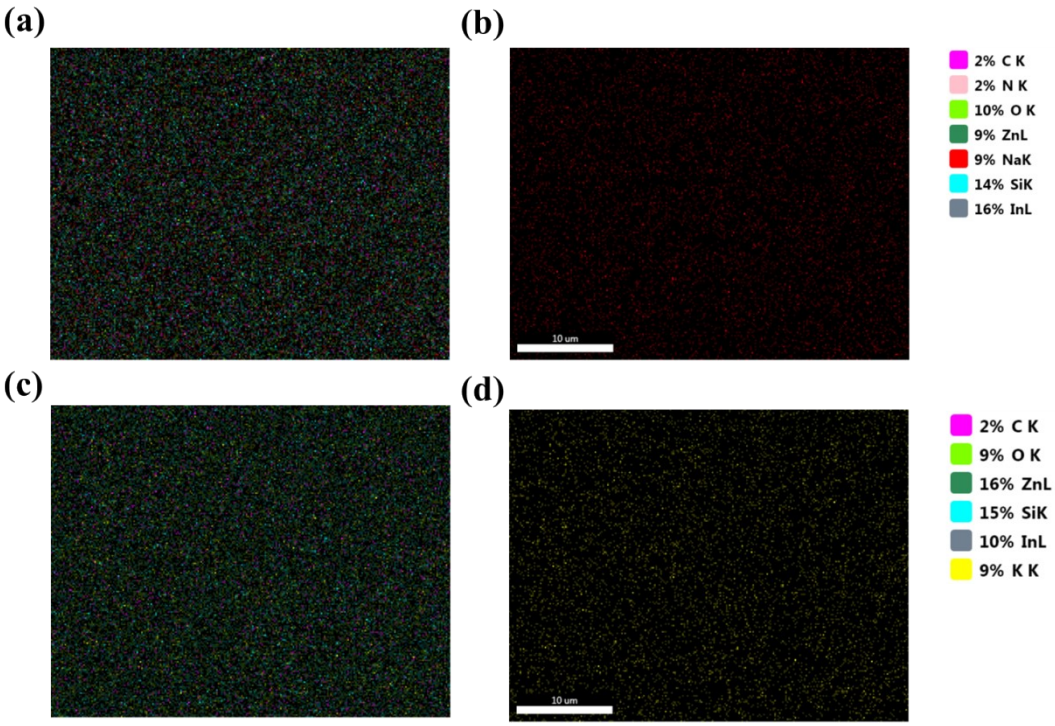

Fig. S10. EDXS mapping images for ITO/ZnO/Ir-Na^+ films for (a) all elements and (b) Na. EDXS mapping images for ITO/ZnO/Ir-K^+ films for (c) all elements and (d) K.

EDXS was proceeded to confirm the ions change in sulfonyl group for Na and K in films, structure of ITO/ZnO/Ir-Na^+ or Ir-K^+. Silicon (Si), Indium (In), and Zinc (Zn) peaks are coming from the other layers (Glass, ITO, and ZnO). We found that other cations (Cs, K, and Li) are not detected in films with Ir-Na^+ through EDXS measurement (Also, Na ion are not detected in films with Ir-K^+). We also analyze the ITO/ZnO/Ir-Li^+ films by EDXS measurement, but Li ions are not detected because of instrumental limitation.

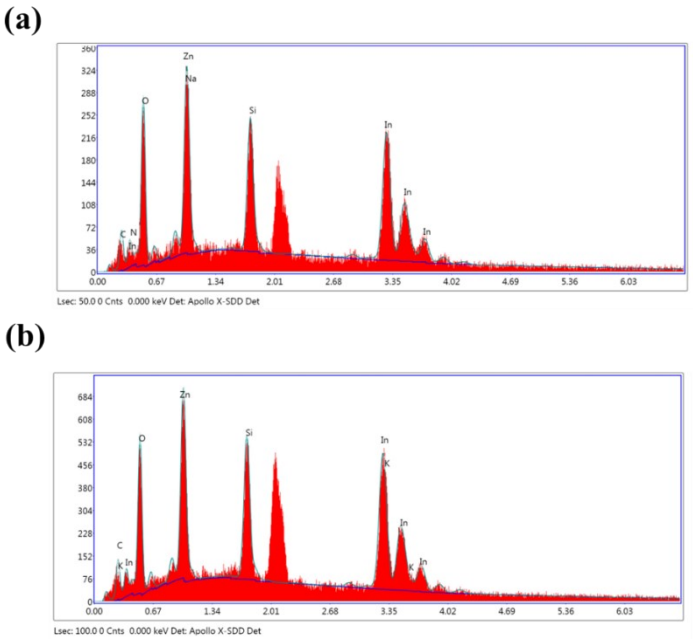

Fig. S11. EDXS data for (a) ITO/ZnO/Ir-Na^+ film and (b) ITO/ZnO/Ir-K^+ film.

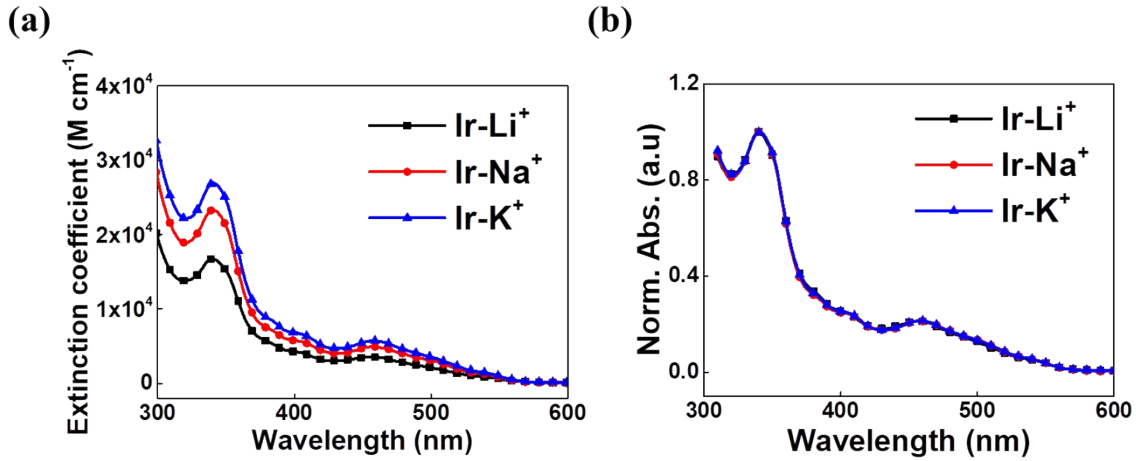

Fig. S12. (a) Extinction coefficient of Ir-Li^+, Ir-Na^+, and Ir-K^+ 0.02 mM solution in 2-MeTHF. (b) Normalized absorbance of Ir-Li^+, Ir-Na^+, and Ir-K^+ 0.02 mM solution in 2-MeTHF.

2. X-ray diffraction (XRD) analysis

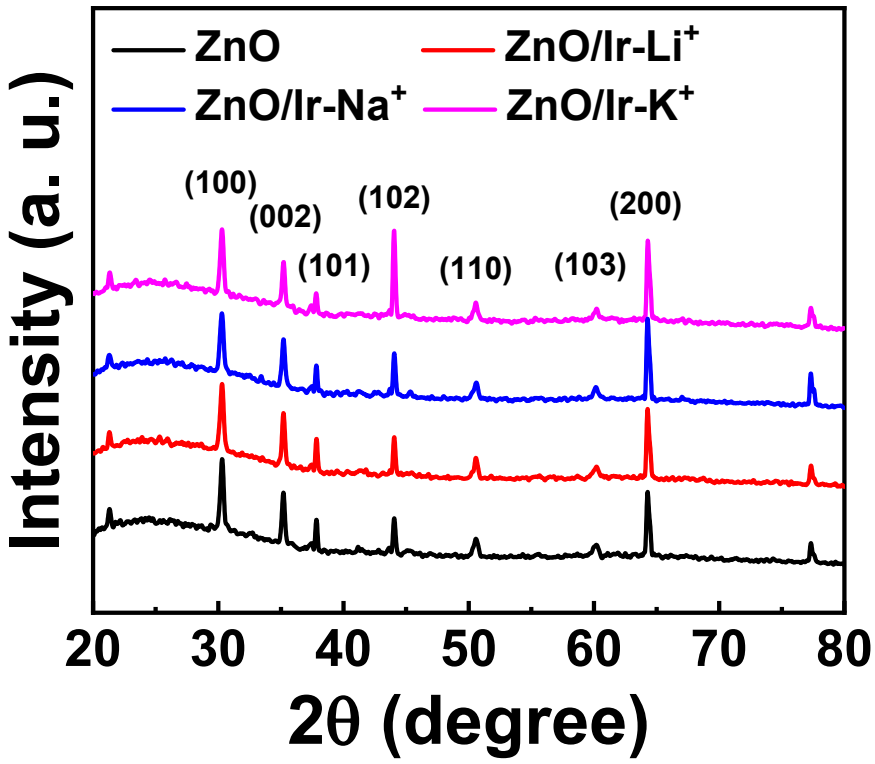

Fig. S13. XRD spectra of ZnO and ZnO/Ir(III) complex films.

XRD spectra show the diffraction peaks of 30.3˚, 35.2˚ and 37.8˚ correspond to the (100), (002) and (101) planes of the ZnO crystal, confirming that formation of the Ir(III) complex layer does not affect to coated ZnO layer.

3. Grazing incidence wide angle X-ray diffraction (GI-WAXD)

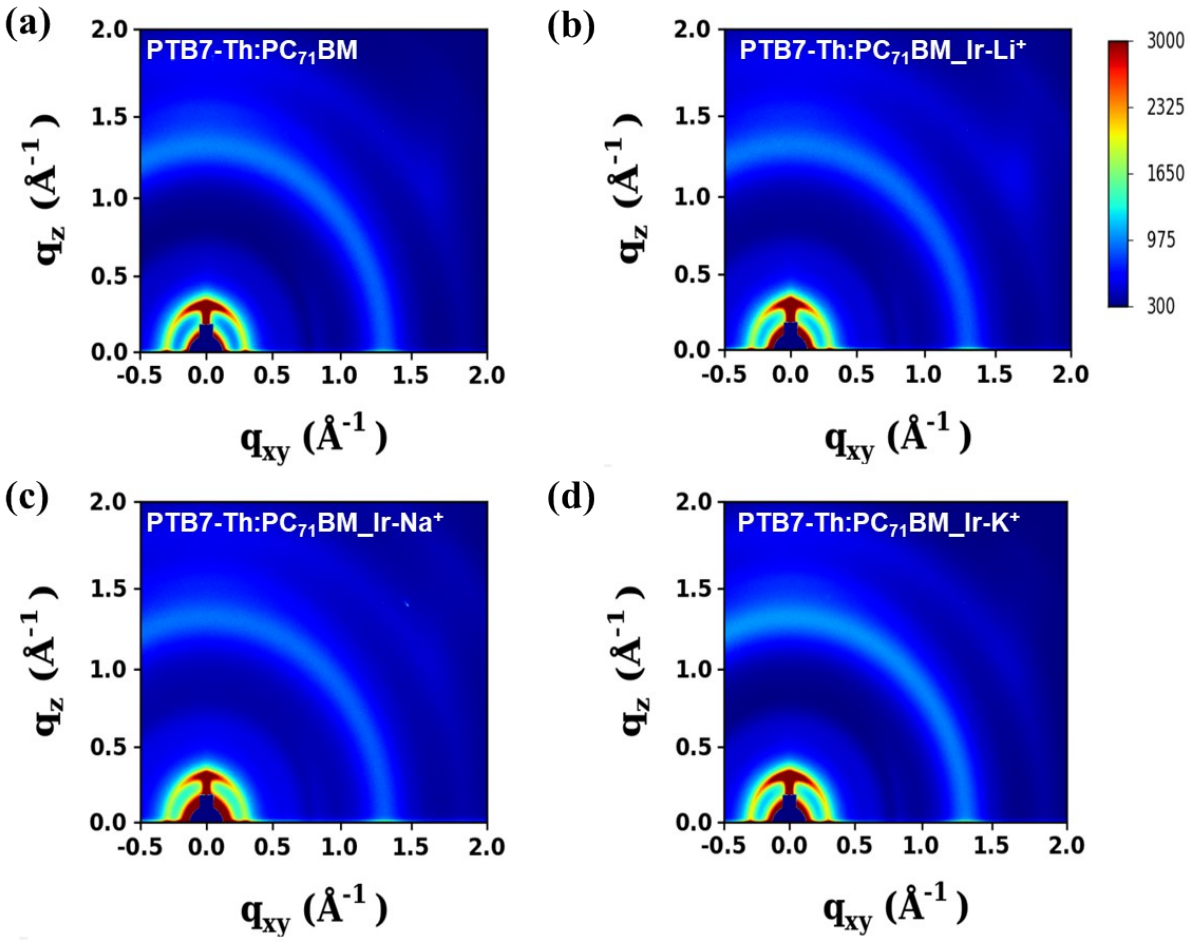

Fig. S14. 2D GI-WAXD images of PTB7-Th:$PC_{71}BM$ films with (a) ZnO layer, (b) ZnO/Ir-Li^+ layer, (c) ZnO/Ir-Na^+ layer and (d) ZnO/Ir-K^+ layer

4. Device performance

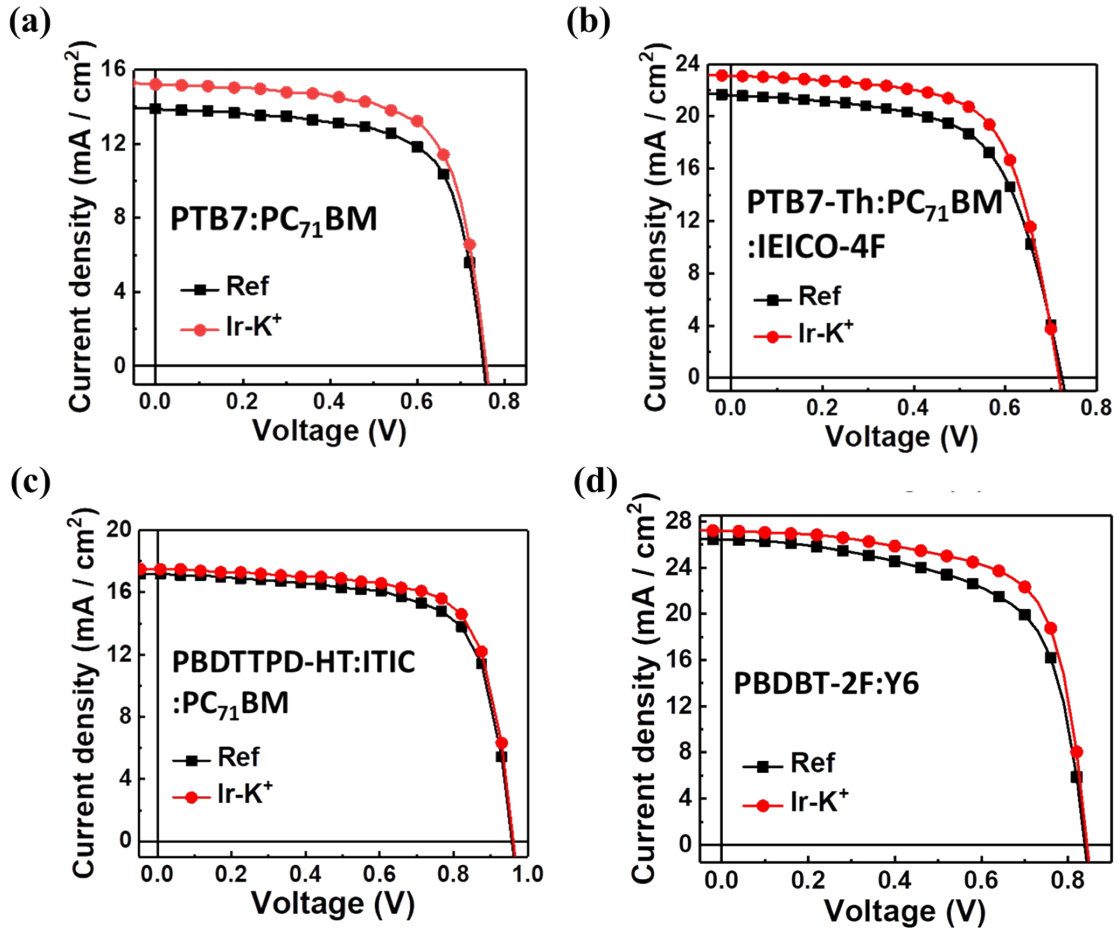

Fig. S15. J-V curves of (a) PTB7:$PC_{71}BM$ blends, (b) PTB7-Th:$PC_{71}BM$:IEICO-4F blends, (c) PBDTTPD-HT:ITIC:$PC_{71}BM$ blends and (d) PBDBT-2F:Y6 blends device with ZnO/Ir-K^+ layer

5. Incident photon to current (IPCE) characteristics

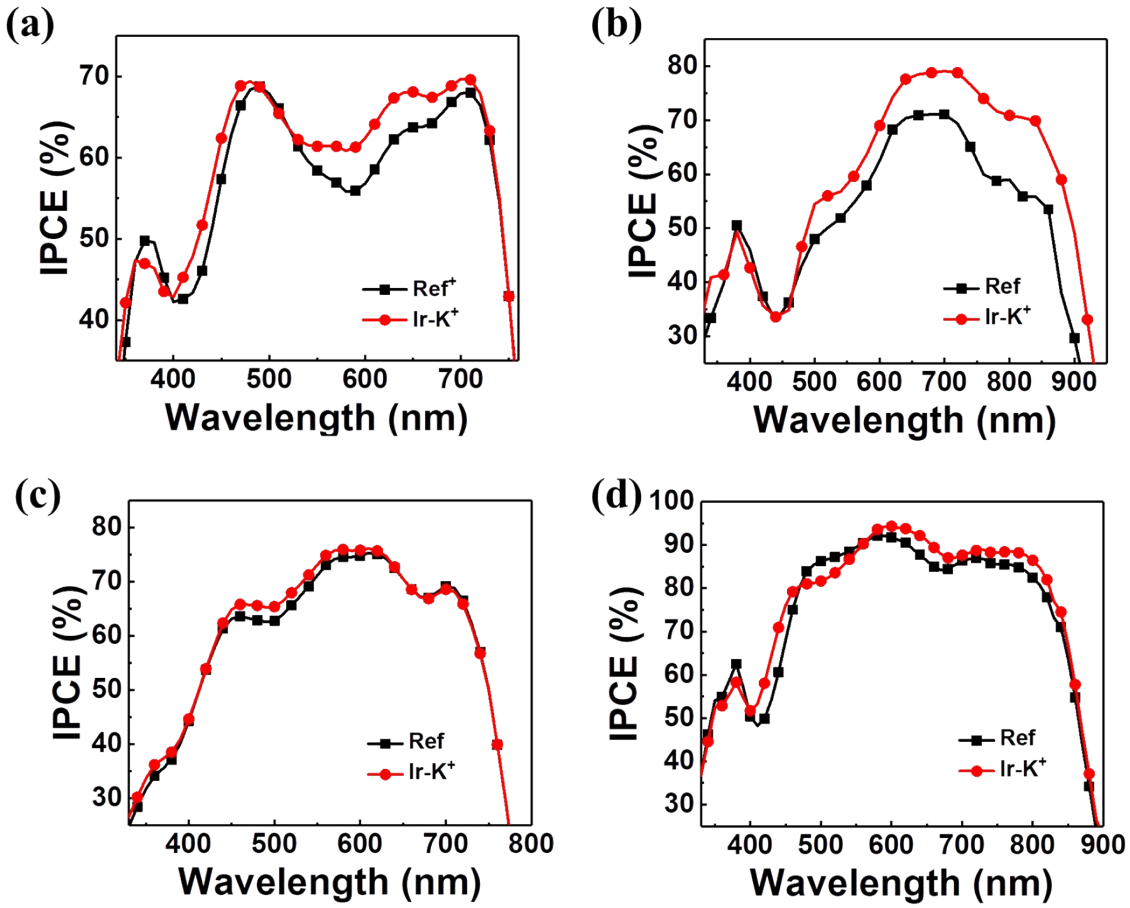

Fig. S16. IPCE characteristics of (a) PTB7:$PC_{71}BM$ blends, (b) PTB7-Th:$PC_{71}BM$:IEICO-4F blends, (c) PBDTTPD-HT:ITIC:$PC_{71}BM$ blends and (d) PBDBT-2F:Y6 blends devices.

.6. Stability test (Under UV illumination)

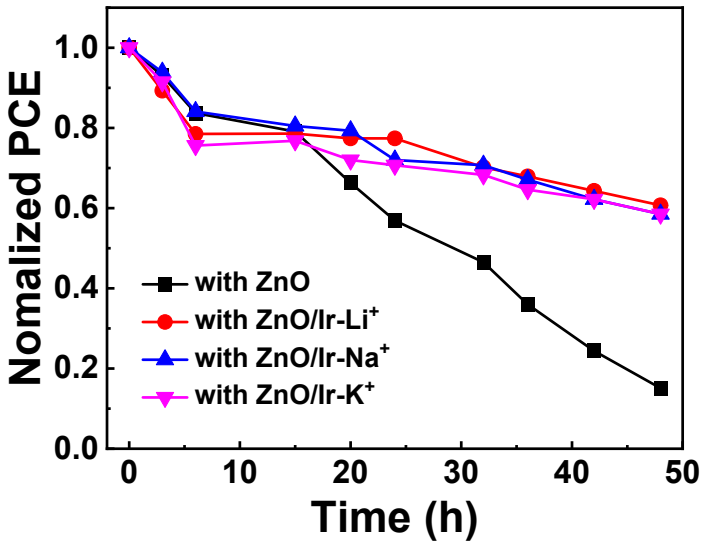

Fig. S17. Stability test under UV illumination with structure of ITO/ZnO/Ir(III) complexes:PEO/PTB7-Th:$PC_{71}BM$/MoO_3/Ag.

7. X-ray photoelectron spectroscopy (XPS) depth profile

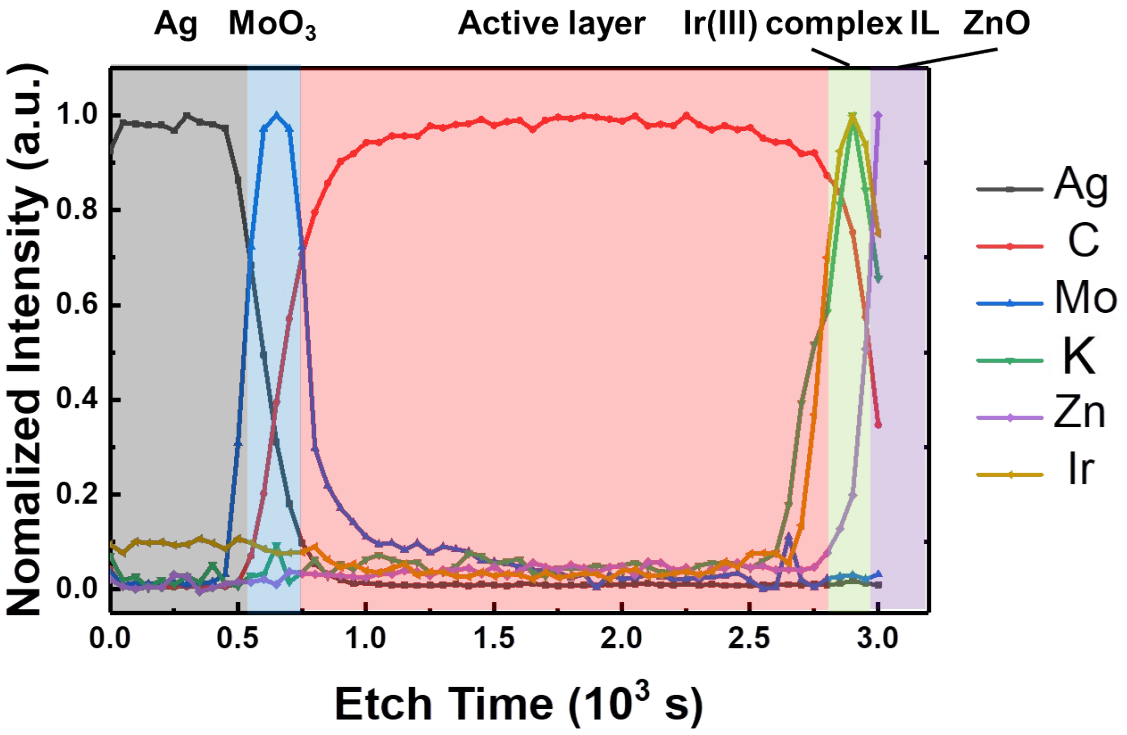

Fig. S18. XPS depth profile of aged device with structure of ITO/ZnO/Ir-K^+:PEO/PTB7-Th:$PC_{71}BM$/MoO_3/Ag under AM 1.5 G irradiation (108 h).

8. UV-aged GI-WAXD images

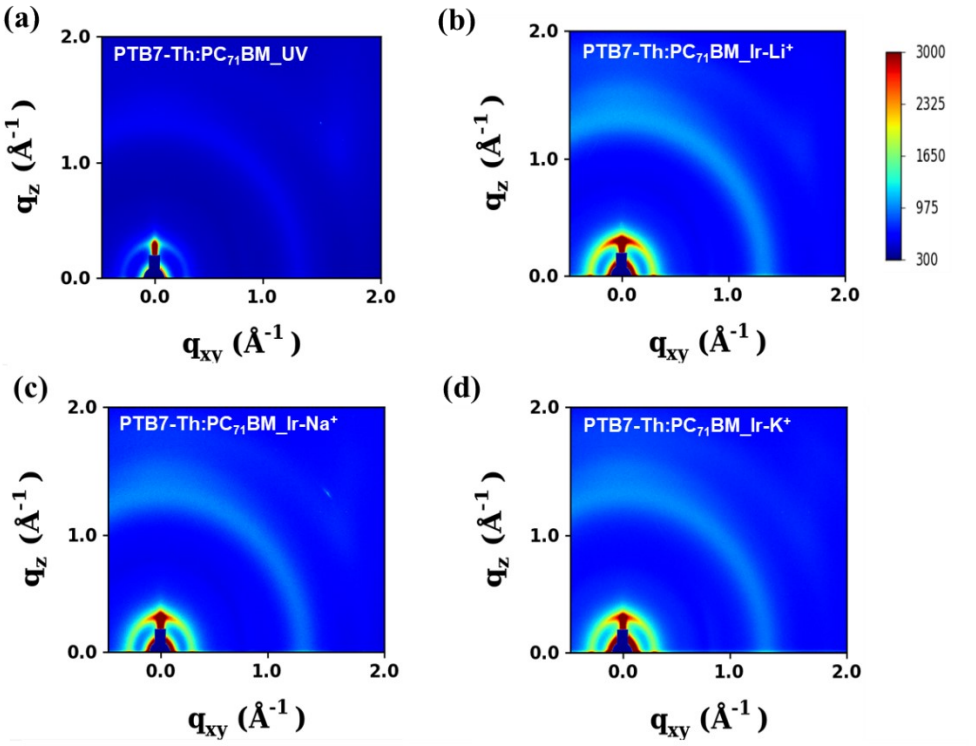

Fig. S19. 2D GI-WAXD images of UV aged PTB7-Th:$PC_{71}BM$ blend films (a) without Ir(III) complex-ILs, (b) with Ir-Li^+ layer, (c) with Ir-Na^+ layer and (d) with Ir-K^+ layer. The aged devices and films were aged under UV light in ambient condition for 48 h before testing (Device structure is ITO/ZnO/Ir(III) complex:PEO/PTB7-Th:$PC_{71}BM$/MoO_3/Ag).

10. Summary tables of properties and performances

Table S1. EDXS data of ITO/ZnO/Ir-Na^+ films.

Element	Weight %	Atomic %	Net Int.	Error %	K ratio	Z	R	A	F
C	4.42	13.74	10.33	16.37	0.02	1.38	0.84	0.33	1
O	19.46	45.45	54.92	12.33	0.06	1.31	0.86	0.24	1
Zn	20.02	11.44	57.23	10.29	0.12	0.95	1.02	0.63	1
Na	1.80	2.92	8.36	29.86	0.01	1.18	0.9	0.41	1
Si	8.42	11.20	67.17	9.12	0.07	1.18	0.92	0.72	1
In	45.75	14.89	88.46	7.33	0.37	0.81	1.1	1.02	1

Table S2. EDXS data of ITO/ZnO/Ir-K^+ films.

Element	Weight %	Atomic %	Net Int.	Error %	K ratio	Z	R	A	F
C	4.66	14.63	11.31	19.40	0.02	1.38	0.84	0.32	1
O	19.04	44.82	57.11	11.28	0.06	1.31	0.86	0.24	1
Zn	21.95	12.65	67.62	7.73	0.13	0.95	1.02	0.64	1
Si	9.02	12.10	76.91	7.22	0.08	1.18	0.92	0.72	1
In	43.85	14.39	90.38	6.63	0.36	0.8	1.1	1.02	1
K	1.47	1.42	6.41	30.02	0.02	1.09	0.96	0.95	1

Table S3. Photo-physical properties of Ir(III) complexes[a]

Material	$\lambda_{max,\ abs(\pi-\pi^*)}$ [nm]	$\lambda_{max,\ abs\ (MLCT)}$ [nm]
Ir-Li^+	340	455
Ir-Na^+	340	455
Ir-K^+	340	455

[a] Photophysical data were determind at room temperature in 2-MeTHF solution.

Table S4. Summary of the PSCs performance with the inverted structure of ITO/ZnO/Ir(III) complex (Ir-Li^+, Ir-Na^+, and Ir-K^+):PEO/active layer/MoO_3/Ag.[a]

Active layer	J_{SC} (mA cm^{-2})	V_{OC} (V)	FF	PCE_{max} (%)
PTB7:$PC_{71}BM$	13.9 (13.7)	0.75 (0.75)	0.68 (0.66)	7.1 (6.8)
PTB7:$PC_{71}BM$_Ir-K^+	15.2 (15.0)	0.76 (0.76)	0.69 (0.68)	8.0 (7.8)
PTB7-Th:$PC_{71}BM$:IEICO-4F	21.6 (21.1)	0.72 (0.72)	0.62 (0.61)	9.8 (9.3)
PTB7-Th:$PC_{71}BM$:IEICO-4F_Ir-K^+	23.1 (22.6)	0.72 (0.72)	0.66 (0.64)	11.0 (10.7)
PBDTTPD-HT:ITIC:$PC_{71}BM$	17.2 (17.2)	0.96 (0.94)	0.69 (0.67)	11.4 (10.9)
PBDTTPD-HT:ITIC:$PC_{71}BM$_Ir-K^+	17.5 (17.2)	0.96 (0.94)	0.72 (0.70)	12.1 (11.4)
PBDBT-2F:Y6	26.4 (25.3)	0.84 (0.82)	0.63 (0.68)	14.0 (14.0)
PBDBT-2F:Y6_Ir-K^+	27.2 (25.7)	0.84 (0.83)	0.68 (0.71)	15.6 (14.9)

[a]The values in brackets are average values of six replicate devices.